

Nonnucleoside Inhibitor Binding Affects the Interactions of the Fingers Subdomain of Human Immunodeficiency Virus Type 1 Reverse Transcriptase with DNA

Elena N. Peletskaya,¹ Alex A. Kogon,² Steven Tuske,³ Edward Arnold,³
and Stephen H. Hughes^{1*}

*HIV Drug Resistance Program*¹ and *SAIC Frederick*,² *National Cancer Institute at Frederick, Frederick, Maryland 21702-1201*, and *Center for Advanced Biotechnology and Medicine, Department of Chemistry and Chemical Biology, Rutgers University, Piscataway, New Jersey 08854-5638*³

Received 4 December 2002/Accepted 25 November 2003

Site-directed photoaffinity cross-linking experiments were performed by using human immunodeficiency virus type 1 (HIV-1) reverse transcriptase (RT) mutants with unique cysteine residues at several positions (i.e., positions 65, 67, 70, and 74) in the fingers subdomain of the p66 subunit. Since neither the introduction of the unique cysteine residues into the fingers nor the modification of the SH groups of these residues with photoaffinity cross-linking reagents caused a significant decrease in the enzymatic activities of RT, we were able to use this system to measure distances between specific positions in the fingers domain of RT and double-stranded DNA. HIV-1 RT is quite flexible. There are conformational changes associated with binding of the normal substrates and nonnucleoside RT inhibitors (NNRTIs). Cross-linking was used to monitor intramolecular movements associated with binding of an NNRTI either in the presence or in the absence of an incoming deoxynucleoside triphosphate (dNTP). Binding an incoming dNTP at the polymerase active site decreased the efficiency of cross-linking but caused only modest changes in the preferred positions of cross-linking. This finding suggests that the fingers of p66 are closer to an extended template in the “open” configuration of the enzyme with the fingers away from the active site than in the closed configuration with the fingers in direct contact with the incoming dNTP. NNRTI binding caused increased cross-linking in experiments with diazirine reagents (especially with a diazirine reagent with a longer linker) and a moderate shift in the preferred sites of interaction with the template. Cross-linking occurred closer to the polymerase active site for RTs modified at positions 70 and 74. The effects of NNRTI binding were more pronounced in the absence of a bound dNTP; pretreatment of HIV-1 RT with an NNRTI reduced the effect of dNTP binding. These observations can be explained if the binding of NNRTI causes a decrease in the flexibility in the fingers subdomain of RT-NNRTI complex and a decrease in the distance from the fingers to the template extension.

Human immunodeficiency virus type 1 (HIV-1), like other retroviruses, has a single-stranded RNA genome that is converted into double-stranded DNA (dsDNA) in the cytoplasm of a newly infected cell. This conversion is carried out by the viral enzyme reverse transcriptase (RT). HIV-1 RT is a homodimeric enzyme composed of two related subunits, p66 and p51. p66 folds into two domains: polymerase and RNase H. The polymerase domain of p66 is divided into four subdomains: fingers, palm, thumb, and connection. p51 contains the first 440 amino acids of p66. This corresponds closely, but not exactly, to the polymerase domain. p51 contains the same four subdomains as the polymerase subdomain, but the relative arrangement of the subdomains is different in p66 and p51. The polymerase and RNase H active site are in the p66 subunit; the role of p51 is primarily structural.

There are a number of different types of structures of HIV-1 RT available. These include the structures of unliganded HIV-1 RT (17, 36); RT bound to a DNA-DNA substrate (7, 20, 21), to a pseudoknot RNA inhibitor (22), and to an RNA-DNA substrate (38). The structure of a ternary complex with a DNA-

DNA substrate and an incoming deoxynucleoside triphosphate (dNTP) has also been determined (18, 19). Several structures of RT-nonnucleoside RT inhibitor (NNRTI) complexes have been published (6, 8, 9, 11, 12, 14–16, 24, 30, 31, 33, 34, 39). Comparison of these structures has provided insights into the mechanism of polymerization and evidence for the flexibility of the enzyme. For example, the position of the fingers subdomain of p66 changes when unliganded HIV-1 RT binds a nucleic acid substrate and the fingers move when the incoming dNTP binds at the polymerase active site.

RT is a major target for anti-HIV-1 drugs. There are two classes of anti-RT drugs: nucleoside RT inhibitors (NRTIs) and NNRTIs. Despite the large number of RT-NNRTI structures, the mechanism of action of the NNRTIs is not well understood (for reviews, see references 10, 23, and 28). The NNRTI binding pocket does not exist in the absence of the inhibitor. The binding of an NNRTI is associated with the formation of a hydrophobic pocket, which distorts the region near the polymerase active site. The binding of different NNRTIs has similar, although not identical, effects on the structure of HIV-1 RT (see supplemental material, which includes a comparison of five different NNRTI-bound RT structures [<http://www.retrovirus.info/rt/>]). Unfortunately, there are no structures of complexes that contain RT with both a bound nucleic acid substrate and an NNRTI. Enzyme kine-

* Corresponding author. Mailing address: HIV Drug Resistance Program, National Cancer Institute—Frederick, P.O. Box B, Bldg. 538, Rm. 130A, Frederick, MD 21702-1201. Phone: (301) 846-1619. Fax: (301) 846-6966. E-mail: hughes@ncifcrf.gov.

ics has provided useful insights (27, 35, 41). The results of the kinetic experiments suggest that binding of an NNRTI does not decrease the binding of either the nucleic acid substrate or the incoming dNTP; however, the chemical step of DNA synthesis is blocked, most likely due to conformational changes in RT. Kinetic studies suggest that binding of the nucleic acid and/or dNTP to RT increases the effectiveness of some NNRTIs (for example, Efavirenz and Sefavirenz) by enhancing the binding of the inhibitor to a ternary complex of RT (1, 27).

Although there are no structures of NNRTI-HIV-1 RT complexes that have bound nucleic acid, comparisons of the available NNRTI-RT structures (6, 8, 9, 11, 12, 14–16, 24, 30, 31, 33, 34, 39) and RT-nucleic acid complexes (7, 18, 20, 21, 38) suggest how NNRTI binding could affect the structure of an RT-nucleic acid complex. Molecular modeling studies have provided additional insight (25, 26, 32, 40, 42). In addition, we now have structures that show the position of an extended template strand both in the presence and in the absence of a bound dNTP (S. Tuske, S. Sarafianos, A. D. Clark, Jr., J. Ding, L. K. Naeger, K. L. White, M. D. Miller, C. S. Gibbs, P. L. Boyer, P. Clark, G. Wang, B. L. Gaffney, R. A. Jones, D. M. Jerina, S. H. Hughes, and E. Arnold, unpublished data).

Binding an NNRTI leads to displacement of the β 12- β 13 hairpin; the β 12- β 13 hairpin interacts directly with a nucleic acid substrate. It is possible that this causes an alteration in the position of the nucleic acid relative to the protein, which could cause changes in the position of the nucleic acid relative to the polymerase active site. Alternatively, the NNRTI binding site includes residues in the β 9- β 10 hairpin. The β 9- β 10 hairpin carries two of the three active site aspartic acids (D185 and D186). There are also contacts between some NNRTIs and the β 6 strand, which carries the third active-site aspartate (D110). Even a moderate shift in the positions of the active-site aspartic acids could interfere with the chemical step of polymerization. Moreover, since the binding of an NNRTI causes a number of changes in the structure of RT, the effect of NNRTI binding on the chemical step may be the result of several of these changes and not simply the effect of any one of the changes.

In the absence of a crystal structure of HIV-1 RT that contains both a bound NNRTI and bound nucleic acid, we used photoaffinity cross-linking (photocrosslinking) to monitor the structural changes caused by the binding of an NNRTI to an RT-DNA complex. We previously showed that the site-directed photocrosslinking of the fingers subdomain of HIV-1 RT to an extended template can be used to monitor changes in the distance between particular positions on the surface of the protein and a nucleic acid substrate and that we could obtain information about changes in the flexibility of the enzyme

(29). Photocrosslinking experiments in which the cross-linking agents were attached to specific positions (i.e., positions 65, 67, 70, and 74) in the β 3- β 4 loop of the fingers subdomain of p66 and photocrosslinked to the single-stranded extension of the template showed that cross-linking was significantly reduced in ternary complexes compared to binary complexes (29). We show here that NNRTI binding causes increased cross-linking in experiments with diazirine reagents (especially with the diazirine reagent with the longer linker) and, for some positions in the β 3- β 4 loop, NNRTI binding shifts the preferred sites of interaction with the template. Cross-linking occurred closer to polymerase active site for RTs modified at positions 70 and 74. This effect was more pronounced when no dNTP is bound. Pretreatment of RT with an NNRTI reduced the effects of dNTP binding. These observations may be explained by the decreased flexibility in the fingers subdomain of RT-NNRTI complex and/or the decreased distance from the fingers to the template extension.

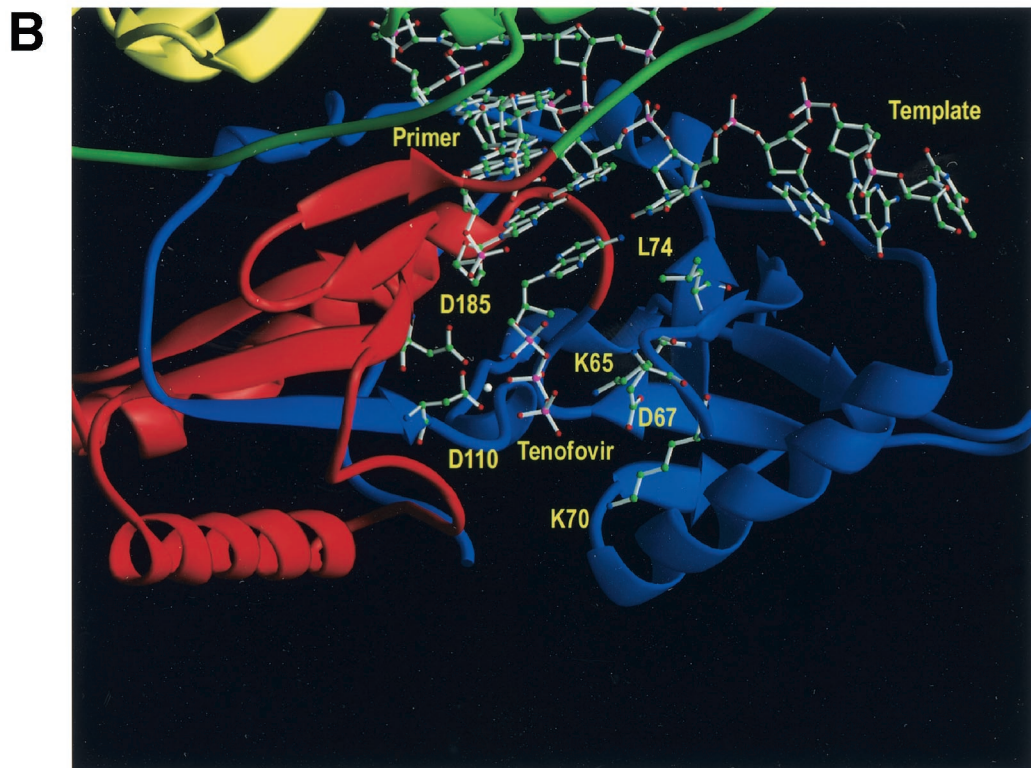
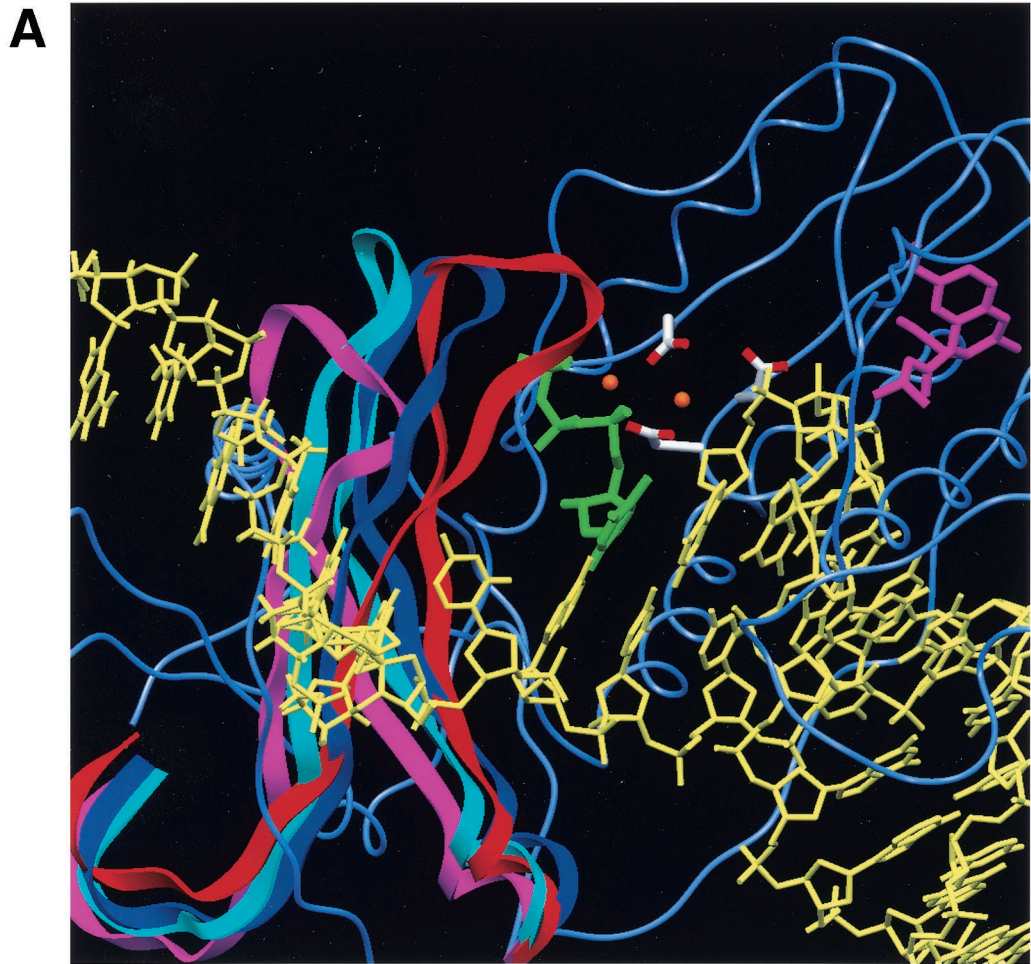
A model based on superimposition of the unliganded, NNRTI-bound, binary and ternary structures (9, 16–18, 37) and new structural information on the position of the extended template (Tuske et al., unpublished) and our photocrosslinking data is shown in Fig. 1. It shows position of β 3- β 4 loop of fingers subdomain that belong to four superimposed X-ray structures of HIV-1 RT: a binary complex with DNA (9), the ternary complex with incoming dNTP and DNA (18), NNRTI HBY 097 complexed with RT (16), unliganded RT (17), and a model of template extended beyond the +3 nucleotide.

MATERIALS AND METHODS

Construction of mutant RT clones. BspMI cassette mutagenesis (4) was used to introduce an ApaI site into the region encoding p66 of HIV-1 RT to make the construct RT (ApaI). This modification does not change the protein sequence of HIV-1 RT but does change the codon usage at Pro52 as follows: -GGG(Gly) CCT(Pro) GAG(Glu)- \rightarrow -GGG(Gly) CCC(Pro) GAG(Glu)-.

The C38V mutation was introduced into each of four plasmids carrying the K65C, D67C, K70C, and L74C mutations, respectively, by using the ApaI site. The plasmids were digested with ApaI/HindIII. The larger fragment from C38V and the smaller fragment from the K65C, D67C, K70C, and L74C mutants were ligated to generate the double mutant. Each of the double mutant plasmids was further modified to produce HIV-1 RT proteins containing the C280S mutation and six histidines at the C terminus. The expression vector pUC12N/p51(-cys) is similar to previously described coexpression vectors (3). The vector contains two *lacZ* promoters oriented in opposite directions. One *lacZ* promoter transcribes a region encoding a p51 subunit with no cysteine residues (the specific mutations are C38V and C280S). The other *lacZ* promoter is oriented toward a polylinker, which contains a unique NcoI site and a unique HindIII site. The plasmids that express only the p66 form of HIV-1 RT from the mutants described above—K65C(-cys)His, D67C(-cys)His, K70C(-cys)His, and L74C(-cys)His—were digested with NcoI/HindIII and cloned into pUC12N/p51(-cys). The resulting plasmids will coexpress the cysteine-less p51 subunit and a p66 subunit with a

FIG. 1. (A) Superimposition of four structures of HIV-1 RT. The solid ribbons show the positions of the β 3- β 4 loop positions in all four structures. The binary complex with DNA (9) (cyan), the ternary complex (red loop and lavender α trace) with incoming dNTP (green) and DNA (yellow) (18), the NNRTI HBY 097 complex with RT (magenta, both the inhibitor and the loop) (16), and unliganded RT (17) (navy blue) are shown. The side chains of amino acid residues of the polymerase active site D110, D185, and D186 of the p66 subunit from the ternary complex are shown. The superimposition was performed by using PROFIT program with five points fixed: two in the polymerase active site, residues 100 to 200 and 400 to 420 of p51, and the RNase H subdomain of p66 (29). The position of the extended template strand was modeled based on the distance constraints that are in agreement with the recent structural data (Tuske et al., unpublished) and the data of our cross-linking experiments. (B) Portion of the ternary structure of HIV-1 RT (Tuske et al., unpublished) with tenofovir showing the portion of the extended template and β 3- β 4 loop. Tenofovir, DNA, and side chains of the active site residues and K65, D67, K70, and L74 are shown in ball-and-stick form colored according to atom type. Portions of the RT are shown as ribbon diagrams colored by subdomain: blue, fingers; green, connection; and red, palm.



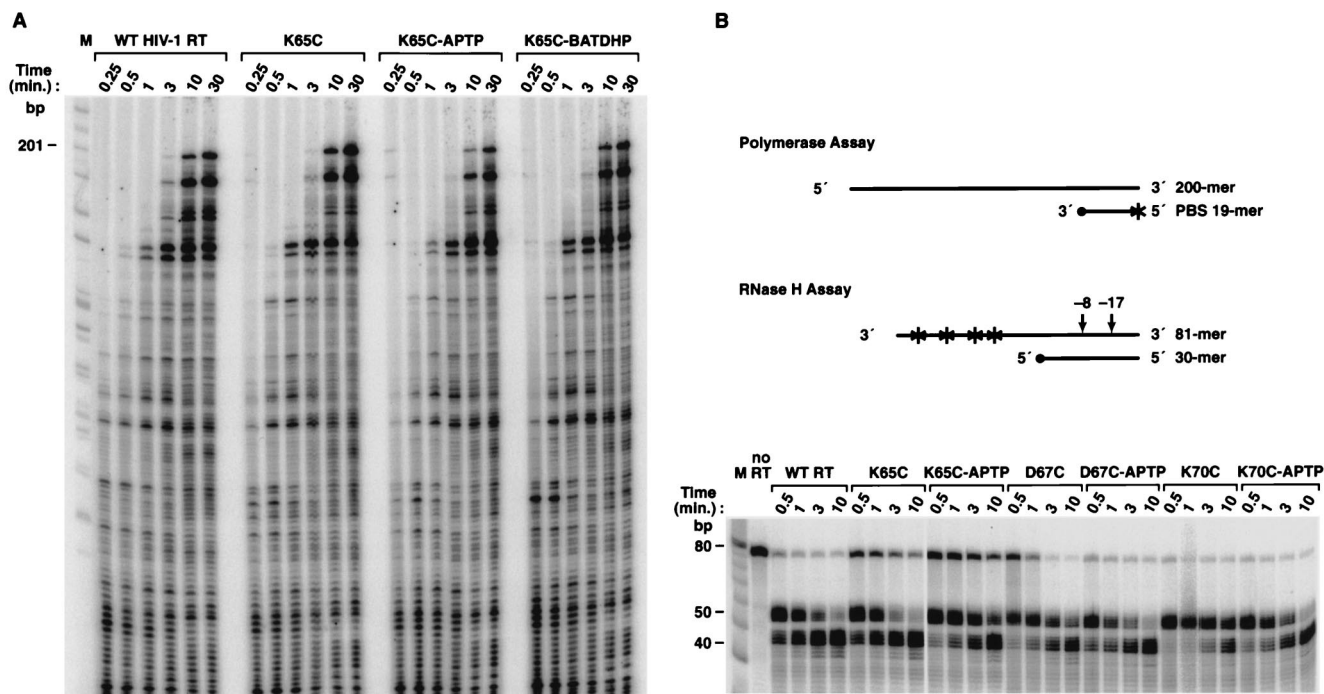


FIG. 2. Enzymatic activities of wild-type and mutant HIV-1 RT with or without photocrosslinker modification. (A) Polymerase activity of wild-type (WT) HIV-1 RT and the K65C mutant (unmodified) and modified with photocrosslinkers APTP and BATDHP. The polymerase assay was performed with a 5'-labeled primer and a 200-base RNA template (shown schematically in panel B) at the top (see also Materials and Methods). The reaction was stopped by the addition of formamide loading buffer at the indicated times (0.25 to 30 min), and the products were fractionated on a 6% denaturing polyacrylamide gel. (B) At the top of the panel is a schematic diagram of the polymerase substrate used in the experiment shown in panel A. In the middle of panel B is the RNase H substrate; the presence of the ^{32}P label in the substrates is indicated by an asterisk. At the bottom of panel B are the results of the RNase H assay. The RNase H activities of wild-type HIV-1 RT (WT), the K65C mutant, the APTP-modified K65C mutant, the D67C mutant, the APTP-modified D67C mutant, the K70C mutant, and APTP-modified K70C mutant are compared. Reactions were performed for periods of time between 0.5 and 10 min. The uncleaved RNA (shown in the "no RT" lane) migrates to a position of about 80 bases. The -17 cleavage produces products about 50 bases long; the -8 cleavage products are about 40 bases long. The reaction was stopped by the addition of formamide loading buffer at the indicated times (0.25 to 30 min), and the products were fractionated on a 15% denaturing polyacrylamide gel.

histidine tail and only one cysteine at the designated site. The six-histidine tag at the C terminus of p66 facilitates protein purification.

Purification of HIV-1 RT. *Escherichia coli* strain DH5 α was transformed with one of the plasmids that express HIV-1 RT described above, and a single colony was picked and inoculated into 750 ml of NZY medium and grown at 37°C for 12 to 14 h before it was harvested by centrifugation. The expression system is based on pUC, so induction is not required for HIV-1 RT expression. The bacterial pellet was washed once with Tris-buffered saline (pH 7.5). The pellet was lysed, and the RT was partially purified on a nickel-chelation affinity agarose column by using the six-histidine tag on the C terminus of p66. Pooled imidazole gradient fractions were dialyzed and then further purified on Q-Sepharose. Purity of the protein preparations was checked by denaturing polyacrylamide gel electrophoresis (PAGE).

Polymerase and RNase H assays. HIV-1 genomic sequences were subcloned from the pNL4-3 clone (2) into the LITMUS 28 plasmid (New England Biolabs, Beverly, Mass.) and sequenced. The R-PBS template RNA was synthesized according to the instructions contained in the Ambion Megashortscript kit (Ambion, Austin, Tex.). In brief, an oligomer containing a T7 promoter, modified so that it contained the sequence for the 5' end of the R region (5'-TACGCCAA GCTACGTAATACGACTCACTATAGGTTCTCTGGTTAGACCAGATCT GAGCCTGGGA-3'), and a second oligomer containing the PBS sequence (5'-AGTCCCTGTTCCGGGCGCCA-3') were used to generate a PCR fragment from the pNL4-3 sequence cloned into LITMUS. The PCR fragment was used as the template for RNA synthesis. RNA was purified by electrophoresis on a 5% denaturing gel, visualized under UV light, and the 200-base band was excised. The gel slice was soaked overnight in a solution of 50 mM Tris (pH 8.0), containing 400 μg of proteinase K (Promega, Madison, Wis.)/ml. The supernatant was recovered, extracted three times with an equal volume of phenol-chloroform, and ethanol precipitated. RNA was quantitated by using a UV spectrophotom-

eter. DNA oligomers were labeled with [γ - ^{32}P]ATP (Amersham Pharmacia, Piscataway, N.J.) and T4 polynucleotide kinase (New England Biolabs).

PBS-R template RNA was mixed with a fivefold molar excess of a ^{32}P -labeled PBS DNA oligonucleotide (5'-AGTCCCTGTTCCGGGCGCCA-3'), followed by incubation at 37°C for 30 min. A threefold molar excess of RT was added to the annealed primer-template and allowed to bind for 1 min at 37°C. Synthesis was initiated by the addition of RT start solution containing dNTPs (80 μM final concentration) and MgCl_2 (6 mM final concentration). Reactions were stopped after appropriate incubation times by the addition of an equal volume of a 90% formamide stop solution containing 1% sodium dodecyl sulfate (SDS), 4 μg of plasmid DNA/ml, bromophenol blue, and xylene cyanole. Reactions were heated to 95°C for 4 min, fractionated by electrophoresis on a denaturing acrylamide gel containing 0.05% SDS, dried under a vacuum, and exposed to a PhosphorImager screen (Molecular Dynamics, Sunnyvale, Calif.). The total amount of DNA synthesized was used as a measure of polymerase activity.

RNase H assays were performed as described earlier (13), the only difference being that there was a twofold excess of RT in the reaction mixtures containing 100 nM RNA-DNA template-primer (Fig. 2).

Photocrosslinkers. Two types of photoactivatable reagents, carbene-generating *N*-bromoacetyl-*N'*-(2,3-dihydroxy-3-[3-(3-(trifluoromethyl)diazirin-3-yl)phenyl]propionyl)ethylenediamine (BATDHP) and *S*-(2-pyridyl)-*S'*-(*N*-[3-(3-(trifluoromethyl)diazirin-3-yl)benzoyl]aminoethyl)disulfide aminoethyl disulfide (PTHBEDS) obtained from Biolinx LLC (Hagerstown, Md.) and a nitrene-generating azide derivative *p*-azidophenylthiophthalimide (APTP) obtained from Sigma (St. Louis, Mo.), were used (Fig. 3). Photocrosslinking reagents were prepared as 10 to 20 mM stock solutions in dimethyl sulfoxide and stored in the dark at -20°C for no longer than 30 days. Carbenes are among the most reactive moieties known. They are capable of reacting with any chemical bond present in a biomolecule, including aliphatic chains and aromatic rings. The reaction times

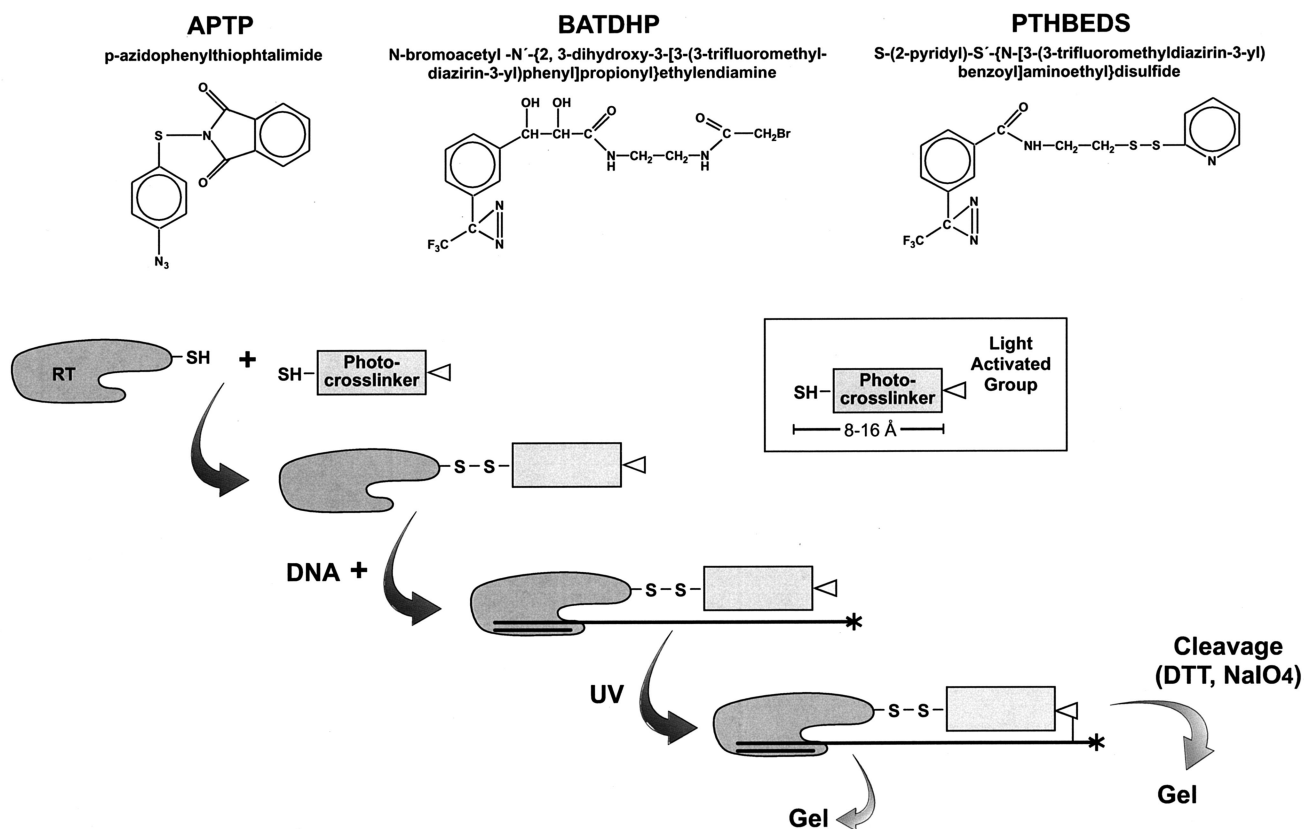


FIG. 3. Photocrosslinking and cleavage reactions of RT and DNA with APTP, BATDHP, and PTHBEDS. These reagents can react specifically with the SH group of a cysteine on RT. In the presence of DNA and UV light, the modified RT can react with DNA. The modified DNA can be released from RT by treatment with DTT in the case of APTP or PTHBEDS, or the vicinal hydroxyls in BATDHP can be selectively cleaved with periodate (IO_4^-). A schematic representation of the reaction of a photocrosslinker with RT and an extended template of a dsDNA is shown below the formulas. The DNA is shown as two lines of unequal length. To monitor the cross-linking reaction, the 5' end of the template was labeled with ^{32}P (*).

for activated carbenes are in the nanosecond range; they form covalent bonds with neighboring atoms nonselectively. Nitrenes, such as those generated from the azide-containing reagent, APTP, are less reactive and tend to undergo intramolecular rearrangements that lead to less-reactive products. These cross-link primarily to nucleophiles such as amino groups and, in a nonnucleophilic environment, can remain active for periods of up to several minutes. This makes them less sensitive for the detection of close interactions. The efficiency of cross-linking with nitrenes formed from azides is higher, but there is a possibility of bias toward reactions with nucleophilic groups.

RT modification. All of the RT mutants were modified with photocrosslinking reagents via a single Cys residue on p66. Next, 50 μl of 1 to 10 μM solutions of RT were treated with 5 mM dithiothreitol (DTT) on ice for 30 min to reduce the SH group. DTT was then removed by gel filtration by using Sephadex G50 Centriscap desalting columns (Princeton Separations, Adelphia, N.J.) in buffer 1 (Tris-Cl [pH 8.0], 60 mM KCl, 10 mM MgCl_2 , 1 mM CHAPS {3-[(3-cholami-

dopropyl)-dimethylammonio]-1-propanesulfonate}). The reduced RT was allowed to react with 10- to 50-fold molar excess of a photoreagent in dark vials on ice for 4 to 12 h. Excess photocrosslinking reagent was removed by gel filtration. All subsequent manipulations were carried at low light levels.

To estimate the extent of SH modification, RT samples were reacted (both before and after modification with thiol-specific cross-linking reagents) with thiol-specific biotin-maleimide (BMCC) from Pierce Co. (Rockford, Ill.) at pH 5.2 according to the manufacturer's instructions. All of the reactions were performed in degassed buffers under argon. Samples were loaded on nonreducing PAGE in 1% SDS and 3 M urea without boiling to avoid non-thiol-specific biotinylation at high pH and high temperatures. Reaction mixtures were analyzed by reacting Western blots with streptavidin conjugated to alkaline phosphatase purchased from Sigma (Fig. 4).

Oligonucleotides. Oligonucleotides were commercially synthesized by using phosphoroamidite chemistry on a synthesizer with subsequent PAGE purifica-

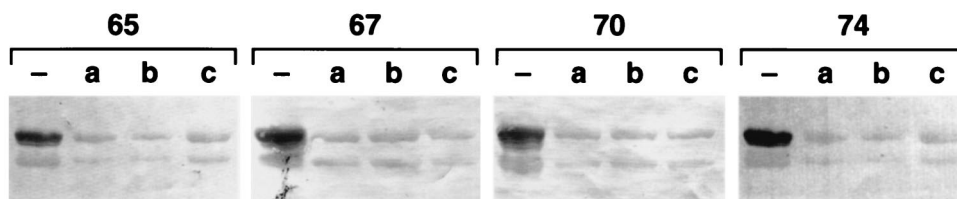


FIG. 4. SH-selective biotinylation of single Cys mutant RTs before and after modification with photocrosslinkers (a “-” symbol stands for a sample biotinylation before modification). The samples biotinylation after modification with photocrosslinking reagents were APTP (lanes a), BATDHP (lanes b), and PTHBEDS (lanes c), respectively. The numbers 65, 67, 70, and 74 represent the K65C, D67C, K70C, and L74C mutant RTs, respectively.

tion (BRL). Oligonucleotides were 5' labeled with [γ - 32 P]ATP and T4 polynucleotide kinase obtained from Boehringer Mannheim and annealed at a 1:1 ratio for cross-linking experiments.

Photocrosslinking. For photocrosslinking, 1 μ M RT and 0.03 μ M template-primer (5' labeled with [γ - 32 P]ATP) were incubated in buffer 1 for 5 min at 37°C and then UV irradiated with a hand-held lamp (model UVM-57; UVP, Upland, Calif.) placed 1 cm away from the samples for 15 min on ice by using a glass plate as an additional filter (cutoff, 315 nm). Nonreducing denaturing PAGE was used to separate the template-primer that was covalently cross-linked to RT. The products were quantified with a PhosphorImager (Storm 860; Molecular Dynamics). The efficiency of cross-linking was calculated as the percentage of radioactivity in the RT-DNA band relative to the total amount of radioactivity in the corresponding lane. Since an excess of RT was used and both the DNA and RT were present at concentrations significantly higher than the RT-DNA binding constant, all of the DNA was assumed to be bound to the enzyme. The negative control samples were obtained by cleaving specific covalent bonds in the cross-linkers. APTP and PTHBEDS cross-links can be cleaved by reducing the disulfide bond formed between the SH groups of the cross-linker and the modified Cys. BATDHP cross-links are cleavable in the presence of 10 mM NaIO₄, which oxidizes a *cis*-diol bond built into the reagent for this purpose.

NNRTIs. The NNRTI used in this project—1-(2,6-difluorobenzyl)-2-(2,6-difluorophenyl)-4-methoxy benzimidazole (M115)—was kindly provided by C. Michejda (NCI-Frederick). A 10 mM stock solution of M115 in dimethyl sulfoxide was stored at -80°C and diluted to 250 μ M with reaction buffer before each experiment, and an appropriate amount of this solution was added to the reaction mixture. The reaction mixtures contained 5 to 50 μ M of M115. We have also used commercial preparations of Efavirenz, 8-Cl TIBO, and α -APA in some experiments and obtained similar results.

RESULTS

We prepared four HIV-1 RT mutants that had the cysteines normally present at positions 38 and 280 replaced in both subunits (by valine and serine, respectively). The mutants each had a single cysteine residue introduced in one of four positions (positions 65, 67, 70, and 74) in the fingers subdomain of the p66 subunit by cassette mutagenesis as described earlier (29). A heterobifunctional photocrosslinker was allowed to react with the cysteine in the fingers subdomain of p66. The efficiency of RT modification by the photocrosslinkers was estimated by biotinylating any remaining free sulfhydryls with biotin maleimide. The biotinylated RT was visualized in a Western blot with streptavidin conjugated to alkaline phosphatase (29). For all three photocrosslinking reagents, ca. 90% of the SH groups on p66 were modified by the photocrosslinking reagents (Fig. 4).

As demonstrated previously, neither the mutations themselves nor the subsequent chemical modification had a major effect on either the polymerase or RNase H activities (29; data not shown [see also Fig. 3]). The inhibition of polymerase activity by 5 μ M M115 was complete for both mutant and modified RTs (data not shown). DNA was allowed to bind to the modified mutant RT, and the complex was irradiated with UV light to activate the photocrosslinker (Fig. 2). We previously showed that all of the mutant RTs that had photocrosslinkers in the fingers of p66 preferentially cross-linked to the template strand of the dsDNA template-primer substrate (29). Therefore, we assumed that, in the protein gels that were used for the subsequent analyses, the majority of the cross-linking was to the template.

The experimental procedures used to determine the localization and efficiency of covalent bond formation between photocrosslinkers on the p66 subunit of HIV-1 RT and the template have been described (29). SH-specific heterobifunctional photoactivatable reagents, the carbene-generating BATDHP

with a linker size of 16 Å, PTHBEDS with a linker size of 11 Å, and the nitrene-generating azide derivative APTP with a linker size of 8 Å were used (Fig. 3; see also Materials and Methods). A number of template-primer pairs were prepared in which the same primer was paired with various templates to create DNA duplexes with 5' template overhangs of 2 to 15 nucleotides. The sequence of the primer matched the primer-binding site of the HIV-1 genome; the 3' end of the primer was a ddNMP. The sequence of the template overhang was a (TG)_n repeat that has no propensity to form secondary structures and no heterogeneity in the sequence. The reaction mixtures containing RT (1 μ M) and template-primer (100 nM) with or without dNTP or NNRTI were incubated 10 min on ice in 10 μ l of buffer 1 in a low-sorption round-bottom 96-well plate. All of the reactions were irradiated simultaneously with UV light (15 min on ice) to ensure equal conditions for all of the parallel experiments. The probability of cross-linking to an extended template is a function of the relative position of the individual amino acid residues and the template overhang; cross-linking can be used to measure the distance between the defined mutant Cys and the template. If there are changes in the relative position of the photocrosslinker and the nucleic acid (for example, upon binding of an NNRTI) the efficiency of cross-linking should be affected. The efficiency of cross-linking to a longer template will always be equal to or greater than the efficiency of cross-linking to a shorter template, since the photocrosslinkers are on flexible arms and have no strong specificity for the bases on the extended templates we have used. Using template extensions of different lengths allows us to estimate where the photocrosslinkers closely approach the nucleic acid. By using three photocrosslinkers with different chemistries and different length flexible arms, we should be able to obtain unambiguous results.

A summary of the results of cross-linking experiments is shown in Fig. 5, where the graphs present the relative yields of photocrosslinking to different template extensions. The experiments to determine the efficiency and the localization of the covalent bond between the fingers of p66 and template extension were performed with binary complexes (RT and dsDNA), with ternary complexes (binary complexes with an incoming dNTP), and with an NNRTI bound either in presence or in absence of an incoming dNTP (Fig. 5). The data presented in Fig. 5 are normalized to simplify the comparisons and the averaging of data from multiple independent experiments. The amount of binary complex cross-linked to TP+11 is set to 100% for each of the modified RTs. The actual maximal yields of cross-linking (generally with TP+11) when only RT and template-primer were present in the cross-linking reactions (binary complex) are shown in Table 1. As expected, the efficiency of cross-linking plateaued as the template was extended. The experiments to determine the efficiency and the location of the covalent bond between the fingers of p66 of RT and template extension were performed with binary complexes, with ternary complexes (binary complexes with an incoming dNTP), and with an NNRTI bound either in the presence or in absence of an incoming dNTP (Fig. 5).

In general, the addition of saturating amounts of NNRTI (up to 40 μ M) caused an increase in the amount of photocrosslinking to the various template extensions for all of the mutants and/or a shift in the preferred sites of interaction

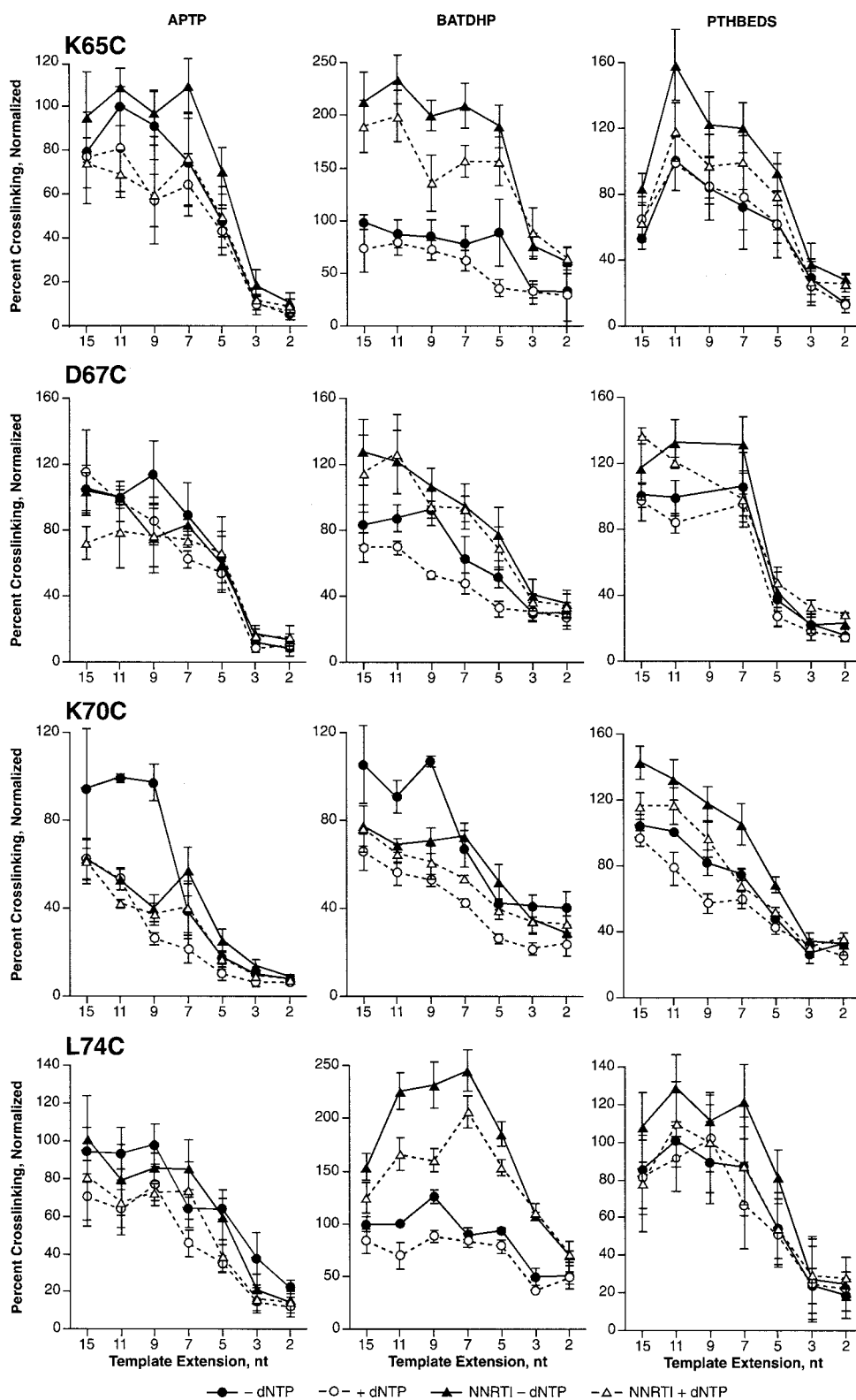


FIG. 5. Yield of photocrosslinking as a function of template extension length. The average of seven independent experiments is plotted, and error is calculated as the standard deviation. The relative yield was calculated as follows: (the percent cross-linking in the RT-TP+11 complex minus the percent cross-linking in a complex of interest/the percent cross-linking in the RT-TP+11 complex) × 100.

TABLE 1. Efficiency of cross-linking HIV-1 RT mutants modified with three different heterobifunctional cross-linking reagents to the DNA template-primer with an 11-nucleotide 5' template overhang

Site of cross-linking	Mean cross-linking efficiency (%) ± SD of cross-linker:		
	APTP (8 Å)	BATDHP (16 Å)	PTHBEDS (11 Å)
K65C	15 ± 3	4 ± 2	5 ± 2
D67C	20 ± 5	4 ± 2	6 ± 2
K70C	7 ± 3	2 ± 1	2 ± 1
L74C	25 ± 8	7 ± 3	8 ± 3

closer to the 3' end of the primer. Most of the experiments were conducted with the NNRTI M115. However, similar results were obtained with other NNRTIs (Efavirenz, 8-Cl TIBO, and α -APA) (data not shown). A number of structures of HIV-1 RT in a simple binary complex with a bound NNRTI have been determined. The different NNRTIs cause similar but not identical changes in the structure of HIV-1 RT (supplemental material, including a comparison of the structures of HIV-1 in complex with five different NNRTIs, is available at <http://www.retrovirus.info/rt/>). It is reasonable to expect that different NNRTIs will also affect the structure of a ternary complex (HIV-1 RT, the NNRTI, and bound nucleic acid) similarly. In general, the efficiency of cross-linking to complexes containing a dNTP and an NNRTI was lower than in complexes that contained an NNRTI but no dNTP; however, the difference in cross-linking was smaller than that caused by the binding of an incoming dNTP in the absence of an NNRTI. The effect of an NNRTI on cross-linking was more pronounced when diazirine reagents were used. When the photocrosslinkers were at positions 65 and 74, the most significant increase in the cross-linking to DNA occurred when an NNRTI was present and BATDHP cross-linkers were used (250% for 65-BATDHP and 150% for 74-BATDHP). PTHBEDS modifications showed 80 and 50% increases for positions 65 and 74, respectively. The larger increase in the amount of cross-linking with BATDHP (16 Å) compared to PTHBEDS (11 Å) and APTP (8 Å) suggested that binding an NNRTI decreases the distance between the fingers of p66 and the extended template but that, even after the fingers have moved, there is still a considerable distance between the fingers and the DNA. APTP-modified RTs showed either moderate increase of cross-linking (65-APTP) combined with a shift of the pre-

ferred interaction sites two to four nucleotides closer to the polymerase active site or only a shift with no increase in the efficiency of cross-linking (67-APTP and 74-APTP). If an NNRTI was present in a complex without a dNTP, 70-APTP cross-linking to DNA was 30% lower and the preferred interactions occurred two nucleotides closer to the polymerase active site. With the dNTP-NNRTI complexes, cross-linking was only 5 to 10% lower than with an NNRTI but no dNTP. In the absence of an inhibitor, dNTP binding decreased cross-linking by ca. 50%, which agrees with our earlier results.

The results of calculations of changes in the yields of cross-linking in different RT-TP complexes relative to the binary complex of each RT mutant with TP11 are summarized in Table 2. The general effect of NNRTI binding on the cross-linking of the fingers of the p66 subunit to an extended DNA template is opposite to the effect of the formation of dNTP-containing closed complexes. If the structures of a binary HIV-1 RT complex that contains an NNRTI and a binary HIV-1 RT complex that contains dsDNA are compared, it is clear that NNRTI binding affects the structural elements of the enzyme that are in contact with the DNA and the incoming dNTP. The position of β 12- β 13, which forms the "roof" of the NNRTI binding pocket, is moved toward the p66 thumb subdomain and in the direction of translocation after nucleotide incorporation; amino acids that are part of β 12- β 13 also make important contacts with bound DNA, and it is possible that these distortions alter the relative positions of the nucleic acid and the protein. However, the binding of the NNRTI causes a number of complex changes in RT, and the possible contributions of these changes are discussed below.

DISCUSSION

The effects of NNRTI binding on photocrosslinking can be interpreted in light of the structure of HIV-1 RT with a bound NNRTI and the structure of HIV-1 RT with a bound nucleic acid. In trying to understand how the cross-linking data correlate with structure, we have focused primarily on the cross-linking experiments for which NNRTI binding (or dNTP binding) had the greatest effect on cross-linking efficiency. We chose to do cross-linking experiments with cross-linking agents using different chemistries and different length linkers in the hope that, in so doing, we could find conditions where there

TABLE 2. Relative change of the yield of photocrosslinking in dsDNA-HIV-1 RT complexes with or without an incoming dNTP in the presence or absence of an NNRTI^a

Cross-linking site	% Relative change in photocrosslinking yield ± SD (shift in nt) with:								
	APTP in the presence (+) or absence (-) of dNTP/NNRTI			BATDHP in the presence (+) or absence (-) of dNTP/NNRTI			PTHBEDS in the presence (+) or absence (-) of dNTP/NNRTI		
	+/-	-/+	+/+	+/-	-/+	+/+	+/-	-/+	+/+
K65C	31 ± 6 (-2)	12 ± 4 (-2)	-30 ± 10 (-2)	-10 ± 3 (+2)	200 ± 50	150 ± 50	-9 ± 5	52 ± 8 (-2)	20 ± 10
D67C	-25 ± 15 (-4)	-20 ± 10	-25 ± 8 (-4)	-31 ± 7	90 ± 50 (-2)	80 ± 50 (-2)	-16 ± 4	38 ± 8	32 ± 9
K70C	-60 ± 10 (+2)	-54 ± 5 (-2)	-61 ± 5 (-2)	-45 ± 5 (+2)	-28 ± 5 (-2)	40 ± 10	-22 ± 8	40 ± 10 (-2)	20 ± 10
L74C	-27 ± 4	-10 ± 10 (-2)	-30 ± 10 (-2)	-32 ± 5	90 ± 30	60 ± 30	-9 ± 7	40 ± 10 (-2)	20 ± 10

^a The relative yield was calculated as described in the text. The results for all the lengths of the template(s) are shown. Extensions were averaged; the numbers represent averages of five to seven independent experiments. Negative numbers in yields indicate decreases in cross-linking efficiency in comparison to the maximum yield for the binary complex without NNRTI. Negative numbers in shifts of preferred position of cross-linking indicate decreases in the number of nucleotides (nt) between the cross-linking site and the end of the primer (site of polymerization); positive numbers indicate increases in this distance in comparison to the distance between the preferred site of cross-linking and the polymerization site in the binary complex of the same mutant.

would be significant differences. It is not surprising for some of the experiments that binding an NNRTI and/or a dNTP caused little, if any, difference in cross-linking. The increased cross-linking seen with the diazirine reagents (BATDHP and PTHBEDS) at positions 65 and 74 when an NNRTI is bound, together with the more moderate increase in cross-linking at position 67, suggests that there is relative movement of the DNA and the fingers of p66. The observation that there is a greater effect on cross-linking with diazirine reagent with the longer cross-linker (BATDHP, 16 Å) suggests that the fingers still are 10 to 15 Å from the extended template.

Our previous efforts to interpret the data on the cross-linking of the extended template and the fingers of p66 were limited because the published structures do not provide much information about the exact location of the extended template. Based on a structure of HIV-1 RT in a complex bound to a dsDNA with a one-base template extension, we proposed that the extended template could pass under the fingers of p66 under certain circumstances (29). There are biochemical data that demonstrate an interaction of the template extension and some portion of HIV-1RT; however, these experiments do not clearly define which portion of the enzyme interacts with the template extension (5, 43). Previously, we interpreted the biochemical and cross-linking data as supporting the idea that, in the open configuration, the extended template can interact directly with the β 3- β 4 loop of the p66 fingers (29). New crystallographic data show this idea is not correct (Tuske et al., unpublished; see also Fig. 1).

In the dTTP-bound closed structure reported by Huang et al. (18) the portion of the template extension nearest the active site passes over the back of the fingers rather than running along or under β 3- β 4 (18). Unfortunately, only a short template extension (three bases) was observed in this structure. The biochemical data suggest that the first six to eight bases of the template extension interact with HIV-1 RT (3, 44). Where then does the extended portion of the template contact the enzyme? We have recently been able to determine the path of a 5'-template extension both in the presence and in the absence of an incoming dNTP analog (Tuske et al., unpublished); the coordinates have been deposited in the PDB data bank (1R0A). The extended template runs over the back of the p66 fingers and interacts with the side chains of F61, W24, and K30. In these structures the position of the 5' end of the template extension differs from the position reported by Huang et al. (18) in that our data suggest the 5' portion of the template extension passes along the p66 fingers subdomain close to the α A helix (which contains K30) rather than across the base of the fingers near β 2 as suggested by the structure presented by Huang et al.. The available biochemical data (35, 41) show that a bound NNRTI does not compete with the binding of the nucleic acid substrate or of an incoming dNTP. NNRTI binding interferes with polymerization by blocking the chemical step of DNA synthesis. However, it is not clear how the distortion of RT structure caused by NNRTI binding leads to the failure of the chemical step.

Binding an NNRTI leads to displacement of the β 12- β 13 hairpin; the β 12- β 13 hairpin interacts directly with a nucleic acid substrate. It is possible that this causes an alteration in the position of the nucleic acid relative to the protein, which could cause changes in the position of the nucleic acid relative to the

TABLE 3. Distances from the C β atoms of amino acid residues 65, 67, 70, and 74 of the β 3- β 4 loop of the HIV-1 RT to the bases of the corresponding nucleotides of the extended template^a

Amino acid (C β)	Distance (Å) to amino acid of nucleotide:											
	T+4			T+3			T+2			T+1		
	a	b	c	a	b	c	a	b	c	a	b	c
K65	17	13	16	16	15	14	13	9	12	11	13	11
D67	20	17	20	20	18	19	17	12	20	17	16	14
K70	19	16	17	17	17	16	16	13	14	15	14	16
L74	15	11	14	11	8	9	11	8	8	6	5	5

^a T+1 is the first unpaired nucleotide closest to the polymerase active site of binary complex, and T+4 is the 5'-most residue). The distances were measured in the X-ray structures (personal communication from Tuske et al. [unpublished] and our model [29]). a, ternary complex; b, binary complex; c, ternary complex in the model.

polymerase active site. Alternatively, the NNRTI binding site includes residues (Y181 and Y188) in the β 9- β 10 hairpin. The β 9- β 10 hairpin carries two of the three active-site aspartic acids (D185 and D186). There are also contacts between some NNRTIs and the β 6 strand that carries the third active-site aspartate (D110). Even a moderate shift in the positions of the active-site aspartic acids could interfere with the chemical step of polymerization. Moreover, since the binding of an NNRTI causes a number of changes in the structure of RT, the effect of NNRTI binding on the chemical step may be the result of several of these changes and not simply the effect of any one of the changes.

There is substantial movement in the fingers subdomain of the p66 subunit of HIV-1 RT when the enzyme binds nucleic acid and then the incoming dNTP. Compared to unliganded HIV-1 RT, the binding of an NNRTI also affects the position of the fingers subdomain (supplementary material, including a comparison of the structures of HIV-1 RT bound to substrates and inhibitors, is available at <http://www.retrovirus.info/rt/>). The movements of the fingers relative to the nucleic acid affects the efficiency of photocrosslinking.

The efficiency of cross-linking of an extended template and the p66 fingers is reduced when an incoming dNTP is bound, creating a closed complex. Since we now know that the trajectory of the template extension is changed only minimally by the formation of the closed complex, the simple interpretation of the photocrosslinking data agrees with the structural data: the fingers of p66 move away from the template during the formation of the closed complex. This is clearly demonstrated in Fig. 1B and Table 3. If we assume that the binding of an NNRTI has a minimal effect on the trajectory of the 5' template extension, the fact that the efficiency of photocrosslinking (especially with BATDHP-modified RTs) is enhanced when an NNRTI is bound suggests that NNRTI binding causes the fingers to move closer to the template extension. The observation that the differences in efficiency are greatest for the photocrosslinker with the long linker extension also suggests that the distance between the derivatized amino acids and the template extension is fairly large (approximately the length of the linker, 16 Å) which agrees with the model.

If we compare the positions of the fingers in the nucleic acid binary complex (RT bound only to nucleic acid) to the position of the fingers in the ternary or closed complex, and with a

bound NNRTI, the movement of the fingers is correlated with the photocrosslinking efficiency. If we also assume that NNRTI binding has a similar effect on the position of the fingers in the presence and in the absence of bound nucleic acid, then the effect of NNRTI binding on the efficiency of photocrosslinking also makes sense: NNRTI binding would move the β 3- β 4 loop closer to extended template (Fig. 1).

The data we obtained by doing photocrosslinking experiments provides a measure of relative distances between specific points on the surface of the protein and the extended template. When these cross-linking efficiencies change, the distance between the protein and the nucleic acid has changed. However, we cannot be sure when an NNRTI binds whether the nucleic acid has moved relative to the β 3- β 4 loop or whether the β 3- β 4 loop has moved relative to the protein. Since we already know, based on crystallographic structures, that the β 3- β 4 loop does move in response to both NNRTI and to dNTP binding and that the extended template does not move when an dNTP binds, we have assumed that it is the movement of β 3- β 4 that is primarily responsible for the differences in photocrosslinking efficiency we have seen.

When both an incoming dNTP and an NNRTI are bound, there presumably are conflicting pressures on the fingers subdomain; the presence of the bound dNTP acting to cause the fingers to close, the NNRTI opposing complete closure of the fingers. The photocrosslinking data suggest that when both the NNRTI and a dNTP are bound, both affect the position of the β 3- β 4 loop. At position 70, it would appear, based on the APTP and BATDHP data, that the effects of dNTP binding predominates, suggesting that, in the complex that contains both a bound NNRTI and a bound dNTP, the portion of β 3- β 4 containing K70 moves to approximately the position it occupies in the normal closed structure in the absence of an NNRTI. Conversely, the cross-linking data (particularly the BATDHP data) suggest that the effects of NNRTI binding predominate over dNTP binding at positions 65 and 74. This suggests that the fingers may not entirely close if both a dNTP and an NNRTI are bound to HIV-1 RT. These data suggest an alternate possibility for the mechanism of NNRTI action: NNRTI binding interferes with the proper closure of the fingers of p66; if the fingers do not close properly, the enzyme cannot carry out the catalytic step.

This proposal is compatible with what we know from the biochemical data; NNRTI binding does not interfere with nucleic acid and/or dNTP binding (35, 41). Both the nucleic acid and the incoming dNTP bind to RT in which the fingers are in the open configuration. Presumably, proper closure of the fingers is important for the positioning of the dNTP and the primer relative to the polymerase active site to allow the chemical step of DNA synthesis to be carried out. If the binding of an NNRTI interferes with the proper closure of the fingers subdomain, this could affect the ability of the fingers to properly align the dNTP and the end of the primer relative to the polymerase active site, which would interfere with the chemical step of DNA synthesis.

ACKNOWLEDGMENTS

We are grateful to C. Michejda for the NNRTI inhibitors used in this project, V. Pletnev for help with graphical presentation of the

molecular model, and Hilda Marusiodis for help in manuscript preparation.

This research was supported by the NCI, NIGMS, and NIAID grants GM56690 and AI27690 to E.A. and NRSA grant AI50338-02 to S.T.

REFERENCES

- Althaus, I. W., J. J. Chou, A. J. Gonzales, M. R. Deibel, K. C. Chou, F. J. Kezdy, D. L. Romero, R. C. Thomas, P. A. Aristoff, W. G. Tarpley, et al. 1994. Kinetic studies with the non-nucleoside human immunodeficiency virus type-1 reverse transcriptase inhibitor U-90152E. *Biochem. Pharmacol.* **47**: 2017–2028.
- Benn, S., R. Rutledge, T. Folks, J. Gold, L. Baker, J. McCormick, P. Feorino, P. Piot, T. Quinn, and M. Martin. 1985. Genomic heterogeneity of AIDS retroviral isolates from North America and Zaire. *Science* **230**:949–951.
- Boyer, P. L., J. Ding, E. Arnold, and S. H. Hughes. 1994. Subunit specificity of mutations that confer resistance to nonnucleoside inhibitors in human immunodeficiency virus type 1 reverse transcriptase. *Antimicrob. Agents Chemother.* **38**:1909–1914.
- Boyer, P. L., A. L. Ferris, and S. H. Hughes. 1992. Cassette mutagenesis of the reverse transcriptase of human immunodeficiency virus type 1. *J. Virol.* **66**:1031–1039.
- Boyer, P. L., C. Tantillo, A. Jacobo-Molina, R. G. Nanni, J. Ding, E. Arnold, and S. H. Hughes. 1994. Sensitivity of wild-type human immunodeficiency virus type 1 reverse transcriptase to dideoxynucleotides depends on template length; the sensitivity of drug-resistant mutants does not. *Proc. Natl. Acad. Sci. USA* **91**:4882–4886.
- Das, K., J. Ding, Y. Hsiou, A. D. Clark, Jr., H. Moereels, L. Koymans, K. Andries, R. Pauwels, P. A. Janssen, P. L. Boyer, P. Clark, R. H. Smith, Jr., M. B. Kroeger Smith, C. J. Michejda, S. H. Hughes, and E. Arnold. 1996. Crystal structures of 8-Cl and 9-Cl TIBO complexed with wild-type HIV-1 RT and 8-Cl TIBO complexed with the Tyr181Cys HIV-1 RT drug-resistant mutant. *J. Mol. Biol.* **264**:1085–1100.
- Ding, J., K. Das, Y. Hsiou, S. G. Sarafianos, A. D. Clark, Jr., A. Jacobo-Molina, C. Tantillo, S. H. Hughes, and E. Arnold. 1998. Structure and functional implications of the polymerase active site region in a complex of HIV-1 RT with a double-stranded DNA template-primer and an antibody Fab fragment at 2.8 Å resolution. *J. Mol. Biol.* **284**:1095–1111.
- Ding, J., K. Das, H. Moereels, L. Koymans, K. Andries, P. A. Janssen, S. H. Hughes, and E. Arnold. 1995. Structure of HIV-1 RT/TIBO R 86183 complex reveals similarity in the binding of diverse nonnucleoside inhibitors. *Nat. Struct. Biol.* **2**:407–415.
- Ding, J., S. H. Hughes, and E. Arnold. 1997. Protein-nucleic acid interactions and DNA conformation in a complex of human immunodeficiency virus type 1 reverse transcriptase with a double-stranded DNA template-primer. *Biopolymers* **44**:125–138.
- Drake, S. M. 2000. NNRTIs: a new class of drugs for HIV. *J. Antimicrob. Chemother.* **45**:417–420.
- Esnouf, R. M., J. Ren, E. F. Garman, D. O. Somers, C. K. Ross, E. Y. Jones, D. K. Stammers, and D. I. Stuart. 1998. Continuous and discontinuous changes in the unit cell of HIV-1 reverse transcriptase crystals on dehydration. *Acta Crystallogr. D Biol. Crystallogr.* **54**:938–953.
- Esnouf, R. M., J. Ren, A. L. Hopkins, C. K. Ross, E. Y. Jones, D. K. Stammers, and D. I. Stuart. 1997. Unique features in the structure of the complex between HIV-1 reverse transcriptase and the bis(heteroaryl)piperazine (BHAP) U-90152 explain resistance mutations for this nonnucleoside inhibitor. *Proc. Natl. Acad. Sci. USA* **94**:3984–3989.
- Gao, H. Q., S. G. Sarafianos, E. Arnold, and S. H. Hughes. 1999. Similarities and differences in the RNase H activities of human immunodeficiency virus type 1 reverse transcriptase and Moloney murine leukemia virus reverse transcriptase. *J. Mol. Biol.* **294**:1097–1113.
- Hopkins, A. L., J. Ren, R. M. Esnouf, B. E. Willcox, E. Y. Jones, C. Ross, T. Miyasaka, R. T. Walker, H. Tanaka, D. K. Stammers, and D. I. Stuart. 1996. Complexes of HIV-1 reverse transcriptase with inhibitors of the HEPT series reveal conformational changes relevant to the design of potent non-nucleoside inhibitors. *J. Med. Chem.* **39**:1589–1600.
- Hopkins, A. L., J. Ren, H. Tanaka, M. Baba, M. Okamoto, D. I. Stuart, and D. K. Stammers. 1999. Design of MKC-442 (emivirine) analogues with improved activity against drug-resistant HIV mutants. *J. Med. Chem.* **42**: 4500–4505.
- Hsiou, Y., K. Das, J. Ding, A. D. Clark, Jr., J. P. Kleim, M. Rosner, I. Winkler, G. Riess, S. H. Hughes, and E. Arnold. 1998. Structures of Tyr188Leu mutant and wild-type HIV-1 reverse transcriptase complexed with the non-nucleoside inhibitor HBY 097: inhibitor flexibility is a useful design feature for reducing drug resistance. *J. Mol. Biol.* **284**:313–323.
- Hsiou, Y., J. Ding, K. Das, A. D. Clark, Jr., S. H. Hughes, and E. Arnold. 1996. Structure of unliganded HIV-1 reverse transcriptase at 2.7 Å resolution: implications of conformational changes for polymerization and inhibition mechanisms. *Structure* **4**:853–860.
- Huang, H., R. Chopra, G. L. Verdine, and S. C. Harrison. 1998. Structure of

- a covalently trapped catalytic complex of HIV-1 reverse transcriptase: implications for drug resistance. *Science* **282**:1669–1675.
19. **Huang, H., S. C. Harrison, and G. L. Verdine.** 2000. Trapping of a catalytic HIV reverse transcriptase template:primer complex through a disulfide bond. *Chem. Biol.* **7**:355–364.
 20. **Jacobo-Molina, A., A. D. Clark, Jr., R. L. Williams, R. G. Nanni, P. Clark, A. L. Ferris, S. H. Hughes, and E. Arnold.** 1991. Crystals of a ternary complex of human immunodeficiency virus type 1 reverse transcriptase with a monoclonal antibody Fab fragment and double-stranded DNA diffract x-rays to 3.5 Å resolution. *Proc. Natl. Acad. Sci. USA* **88**:10895–10899.
 21. **Jacobo-Molina, A., J. Ding, R. G. Nanni, A. D. Clark, Jr., X. Lu, C. Tantillo, R. L. Williams, G. Kamer, A. L. Ferris, P. Clark, A. Hizi, S. H. Hughes, and E. Arnold.** 1993. Crystal structure of human immunodeficiency virus type 1 reverse transcriptase complexed with double-stranded DNA at 3.0 Å resolution shows bent DNA. *Proc. Natl. Acad. Sci. USA* **90**:6320–6324.
 22. **Jaeger, J., T. Restle, and T. A. Steitz.** 1998. The structure of HIV-1 reverse transcriptase complexed with an RNA pseudoknot inhibitor. *EMBO J.* **17**:4535–4542.
 23. **Katlama, C.** 1999. Review of NNRTIs: “today and tomorrow.” *Int. J. Clin. Pract. Suppl.* **103**:16–20.
 24. **Kohlstaedt, L. A., J. Wang, J. M. Friedman, P. A. Rice, and T. A. Steitz.** 1992. Crystal structure at 3.5 Å resolution of HIV-1 reverse transcriptase complexed with an inhibitor. *Science* **256**:1783–1790.
 25. **Kroeger-Smith, M. B., C. J. Michejda, S. H. Hughes, P. L. Boyer, P. A. Janssen, K. Andries, R. W. Buckheit, Jr., and R. H. Smith, Jr.** 1997. Molecular modeling of HIV-1 reverse transcriptase drug-resistant mutant strains: implications for the mechanism of polymerase action. *Protein Eng.* **10**:1379–1383.
 26. **Kroeger Smith, M. B., C. A. Rouzer, L. A. Taneyhill, N. A. Smith, S. H. Hughes, P. L. Boyer, P. A. Janssen, H. Moereels, L. Koymans, E. Arnold, J. Ding, K. Das, W. Zhang, C. J. Michejda, and R. H. Smith, Jr.** 1995. Molecular modeling studies of HIV-1 reverse transcriptase nonnucleoside inhibitors: total energy of complexation as a predictor of drug placement and activity. *Protein Sci.* **4**:2203–2222.
 27. **Maga, G., D. Ubiali, R. Salvetti, M. Pregnotato, and S. Spadari.** 2000. Selective interaction of the human immunodeficiency virus type 1 reverse transcriptase nonnucleoside inhibitor efavirenz and its thio-substituted analog with different enzyme-substrate complexes. *Antimicrob. Agents Chemother.* **44**:1186–1194.
 28. **Pedersen, O. S., and E. B. Pedersen.** 1999. Non-nucleoside reverse transcriptase inhibitors: the NNRTI boom. *Antivir. Chem. Chemother.* **10**:285–314.
 29. **Peletskaya, E. N., P. L. Boyer, A. A. Kogon, P. Clark, H. Kroth, J. M. Sayer, D. M. Jerina, and S. H. Hughes.** 2001. Cross-linking of the fingers subdomain of human immunodeficiency virus type 1 reverse transcriptase to template-primer. *J. Virol.* **75**:9435–9445.
 30. **Ren, J., R. Esnouf, E. Garman, D. Somers, C. Ross, I. Kirby, J. Keeling, G. Darby, Y. Jones, and D. Stuart.** 1995. High resolution structures of HIV-1 RT from four RT-inhibitor complexes. *Nat. Struct. Biol.* **2**:293–302.
 31. **Ren, J., R. Esnouf, A. Hopkins, C. Ross, Y. Jones, D. Stammers, and D. Stuart.** 1995. The structure of HIV-1 reverse transcriptase complexed with 9-chloro-TIBO: lessons for inhibitor design. *Structure* **3**:915–926.
 32. **Ren, J., R. M. Esnouf, A. L. Hopkins, D. I. Stuart, and D. K. Stammers.** 1999. Crystallographic analysis of the binding modes of thiazoloisoindolinone non-nucleoside inhibitors to HIV-1 reverse transcriptase and comparison with modeling studies. *J. Med. Chem.* **42**:3845–3851.
 33. **Ren, J., R. M. Esnouf, A. L. Hopkins, J. Warren, J. Balzarini, D. I. Stuart, and D. K. Stammers.** 1998. Crystal structures of HIV-1 reverse transcriptase in complex with carboxanilide derivatives. *Biochemistry* **37**:14394–14403.
 34. **Ren, J., C. Nichols, L. E. Bird, T. Fujiwara, H. Sugimoto, D. I. Stuart, and D. K. Stammers.** 2000. Binding of the second generation non-nucleoside inhibitor S-1153 to HIV-1 reverse transcriptase involves extensive main chain hydrogen bonding. *J. Biol. Chem.* **275**:14316–14320.
 35. **Rittinger, K., G. Divita, and R. S. Goody.** 1995. Human immunodeficiency virus reverse transcriptase substrate-induced conformational changes and the mechanism of inhibition by nonnucleoside inhibitors. *Proc. Natl. Acad. Sci. USA* **92**:8046–8049.
 36. **Rodgers, D. W., S. J. Gamblin, B. A. Harris, S. Ray, J. S. Culp, B. Hellmig, D. J. Woolf, C. Debouck, and S. C. Harrison.** 1995. The structure of unliganded reverse transcriptase from the human immunodeficiency virus type 1. *Proc. Natl. Acad. Sci. USA* **92**:1222–1226.
 37. **Sarafianos, S. G., K. Das, J. Ding, P. L. Boyer, S. H. Hughes, and E. Arnold.** 1999. Touching the heart of HIV-1 drug resistance: the fingers close down on the dNTP at the polymerase active site. *Chem. Biol.* **6**:R137–R146.
 38. **Sarafianos, S. G., K. Das, C. Tantillo, A. D. Clark, Jr., J. Ding, J. M. Whitcomb, P. L. Boyer, S. H. Hughes, and E. Arnold.** 2001. Crystal structure of HIV-1 reverse transcriptase in complex with a polypurine tract RNA: DNA. *EMBO J.* **20**:1449–1461.
 39. **Smerdon, S. J., J. Jager, J. Wang, L. A. Kohlstaedt, A. J. Chirino, J. M. Friedman, P. A. Rice, and T. A. Steitz.** 1994. Structure of the binding site for nonnucleoside inhibitors of the reverse transcriptase of human immunodeficiency virus type 1. *Proc. Natl. Acad. Sci. USA* **91**:3911–3915.
 40. **Smith, M. B., M. L. Lamb, J. Tirado-Rives, W. L. Jorgensen, C. J. Michejda, S. K. Ruby, and R. H. Smith, Jr.** 2000. Monte Carlo calculations on HIV-1 reverse transcriptase complexed with the non-nucleoside inhibitor 8-Cl TIBO: contribution of the L100I and Y181C variants to protein stability and biological activity. *Protein Eng.* **13**:413–421.
 41. **Spence, R. A., W. M. Kati, K. S. Anderson, and K. A. Johnson.** 1995. Mechanism of inhibition of HIV-1 reverse transcriptase by nonnucleoside inhibitors. *Science* **267**:988–993.
 42. **Tantillo, C., J. Ding, A. Jacobo-Molina, R. G. Nanni, P. L. Boyer, S. H. Hughes, R. Pauwels, K. Andries, P. A. Janssen, and E. Arnold.** 1994. Locations of anti-AIDS drug binding sites and resistance mutations in the three-dimensional structure of HIV-1 reverse transcriptase: implications for mechanisms of drug inhibition and resistance. *J. Mol. Biol.* **243**:369–387.
 43. **Tong, W., C. D. Lu, S. K. Sharma, S. Matsuura, A. G. So, and W. A. Scott.** 1997. Nucleotide-induced stable complex formation by HIV-1 reverse transcriptase. *Biochemistry* **36**:5749–5757.
 44. **Wohrl, B. M., M. M. Georgiadis, A. Telesnitsky, W. A. Hendrickson, and S. F. Le Grice.** 1995. Footprint analysis of replicating murine leukemia virus reverse transcriptase. *Science* **267**:96–99.